Sustainable Polymer & Energy

SCIEPublish

Article

Balance Among Biodegradability, Thermal and Mechanical Properties of CO_2-Derived Polymers

Yansong Ren [1], Xuan Zhao [1], Dongmei Han [2], Shuanjin Wang [1], Sheng Huang [1] and Min Xiao [1,*]

[1] The Key Laboratory of Low-Carbon Chemistry & Energy Conservation of Guangdong Province, State Key Laboratory of Optoelectronic Materials and Technologies, School of Materials Science and Engineering, Sun Yat-sen University, 135 Xingang West, Guangzhou 510275, China; renys@mail2.sysu.edu.cn (Y.R.); zhaox237@mail2.sysu.edu.cn (X.Z.); wangshj@mail.sysu.edu.cn (S.W.); huangsh47@mail.sysu.edu.cn (S.H.)

[2] School of Chemical Engineering and Technology, Sun Yat-sen University, Guangzhou 510275, China; handongm@mail.sysu.edu.cn (D.H.)

* Corresponding author. E-mail: stsxm@mail.sysu.edu.cn (M.X.)

Received: 26 March 2026; Revised: 29 April 2026; Accepted: 5 June 2026; Available online: 25 June 2026

ABSTRACT: Research into biodegradable polymers, driven by environmental imperatives, has progressed significantly. The copolymerization of CO_2 and epoxides produces poly(propylene carbonate) (PPC), which exhibits favorable biodegradability but suffers from poor thermomechanical properties. To address this, recent studies have incorporated rigid monomers or crystalline segments into such copolymerizations, generating a diverse range of CO_2-derived copolymers with enhanced thermal and mechanical performance. However, their degradation profiles remain insufficiently characterized. In this study, we selected several representative CO_2-derived copolymers, recently synthesized by our group, to systematically investigate the structure-property relationship. We evaluated their biodegradability through a series of tests, including biodegradation rate analysis, compost disintegration, and seed germination assays. These polymers, developed by our research team, offer advantages such as low cost, tunable properties, broad applicability, and environmental compatibility. They are thus promising candidates for introducing new materials into the biodegradable plastics market.

Keywords: CO_2 utilization; Polycarbonate; Polyester; Copolymerization; Biodegradable; Biodegradation rate

1. Introduction

The advancement of polymer science has led to the widespread integration of plastic products across nearly every sector of modern society [1]. Initially, the development of aliphatic hydrocarbon polymers progressed rapidly. These materials possess highly stable structures and excellent mechanical properties, combining both toughness and strength, which facilitates their transportation and application [2]. However, due to their chemical inertness, the absence of microbial decomposition mechanisms, and limitations imposed by environmental conditions, such plastics are inherently resistant to biodegradation [3–5]. In recent years, research and development in biodegradable plastics have flourished, yielding significant progress [6]. Polymers such as polylactic acid (PLA), polyhydroxyalkanoates (PHA), and poly(butylene

adipate-co-terephthalate) (PBAT) currently represent biodegradable plastics with mature production processes and broad applications. Nevertheless, they continue to face challenges, including high costs, performance limitations, and imperfect recycling systems [7].

The synthesis of polycarbonates through the alternating copolymerization of CO_2 and epoxides has constituted a vibrant field of research for decades. This method not only provides a sustainable pathway for utilizing CO_2, a significant greenhouse gas, but also facilitates the production of innovative polymeric materials. Poly(propylene carbonate) (PPC), a prominent product of this copolymerization, has been successfully developed. Substantial efforts have been directed toward optimizing the catalytic systems and reaction conditions for this process [8–13]. However, despite advantages such as low cost, low energy consumption, CO_2 utilization, and biodegradability, PPC suffers from a low glass transition temperature (T_g) and softening point, which limit its applications. To address these shortcomings, multi-component copolymerization has emerged as a key strategy for enhancing the thermal and mechanical properties of CO_2-derived polycarbonates. This approach involves exploring a wide range of epoxides with diverse chemical structures and reactivities. By incorporating various epoxides and introducing a third monomer, researchers have developed derivative polycarbonates with more tailored properties [14–18]. For instance, the addition of acid anhydrides or cyclic esters to the reaction mixture can yield random or block copolymers [15,19–23]. This technique enables precise control over the polymer's molecular architecture, thereby tuning its physical and chemical characteristics. Furthermore, through the rational design of block structures and the introduction of functional branches, CO_2-derived polymers exhibiting unique properties such as amphiphilicity, thermoplastic elasticity, and electrical conductivity have been reported [12,24,25]. These novel properties expand the potential applications of CO_2-derived polycarbonates into fields such as biomedicine, electronics, and advanced materials science.

Significant progress has been made in developing CO_2-derived biodegradable polymers, with numerous structures and functionalities successfully synthesized. However, a comprehensive and systematic analysis of their biodegradability, supported by robust experimental data, remains limited. Polymers containing hydrolyzable bonds, such as esters and carbonates, are generally amenable to biodegradation. Yet, their sensitivity to hydrolytic agents and their degradation kinetics under acidic or alkaline conditions can vary considerably [26–29]. Since degradation behavior is influenced by multiple factors—including main-chain structure, side-chain composition, steric hindrance, and biotoxicity—experimental determination of specific biodegradation rates is essential.

In previous work, our research group developed a series of biodegradable CO_2-derived polymers, including cost-effective novel polyester-polycarbonate copolymers (PPCP, PPCX) [15,16,30–33]. These materials are designed for potential applications in biodegradable packaging, agricultural mulch films, foam materials, and plasticizers. Notably, hyperbranched-modified PPCP exhibits performance characteristics comparable to those of commercial PLA while offering significant cost-effectiveness [34]. Herein, the biodegradation rates of these polymers were systematically evaluated using a compost degradation model. Sample surface properties and mass changes were monitored at multiple intervals over a defined period. This study aims to systematically elucidate the interactions between CO_2-derived polymers of varying structures and biodegradation enzymes, as well as to establish structure-activity relationships governing their biodegradability. By identifying functional groups associated with high biodegradability, this research provides valuable insights to guide the future design and development of advanced biodegradable materials.

2. Experimental

2.1. Materials

Propylene oxide (PO, Energy, Shanghai, China, 99%) was refluxed over CaH_2 and distilled under N_2. Cyclohexane oxide (CHO, Energy, 98%), phthalic anhydride (PA, Xuyang, Beijing, China, 99%),

Bis(triphenylphosphine) ammonium chloride (PPNCl, Alfa, Shanghai, China, 97%), triethyl borane (TEB, Energy, 1 M in THF), polylactic acid (PLA, Energy, 80,000 Da), Pyromellitic dianhydride (PMDA, Macklin, Shanghai, China, 99%) and high purity CO_2 (Guangqi Gas Co., Ltd., Guangzhou, China, >99.999%) were all purchased and used directly.

2.2. Characterization Methods

^{1}H NMR spectra were recorded on a Bruker DRX-400 MHz NMR spectrometer (Bruker, Germany) using $CDCl_3$ as solvent.

Molecular weight (M_n) and Dispersity (Đ) were determined by a Shimadzu gel permeation chromatography (GPC) system with THF or $CHCl_3$ as the eluent and polystyrene as the standard.

Differential scanning calorimetry (DSC) analysis was performed by a DSC Model 204 (Netzsch, Germany) under nitrogen flow. Samples were heated and cooled at a rate of 20 °C/min. The glass transition temperature (T_g) was measured from the second heating curve.

Thermogravimetric analysis (TG) was carried out with a PerkinElmer Pyris Diamond TG/DTA analyzer (PerkinElmer, Shelton, CT, USA) using nitrogen (150 mL/min) as protective gas. The samples were heated at a rate of 10 °C/min from room temperature to 600 °C.

Vicat softening temperature (VST) was performed by a SANS ZWK 1302-A HDT&Vicat testing machine (SANS, Shenzhen, China). The heating rate of silicone oil was 50 °C/h. When the depth of the needle pressing into the sample surface reaches 1 mm, the temperature at that time is the VST of the sample.

Mechanical properties were characterized on a universal testing machine (CMT 4204, SANS, Shenzhen, China). Samples were prepared as dumbbell-shaped specimens with a size of 25 × 4 × 1 mm for the test. The stretching rate was 10 or 50 mm/min.

The biodegradation rate experiment refers to ISO 14855. The powdered plastic samples are mixed into the compost under 58 ± 2 °C, an air-flow rate of 100–150 mL/min, and a humidity of 50%. A total organic carbon analyzer is employed to determine the CO_2 release amount within 180 days relative to the blank control group.

$$D_t = \frac{S_{CO_2} - B_{CO_2}}{T_{CO_2}} \times 100\%$$

D_t represents the biodegradation rate on the t-th day, S_{CO_2}, B_{CO_2}, T_{CO_2} are the CO_2 release amounts of the sample group, the control group, and the theoretical total release amount, respectively. Both S_{CO_2} and B_{CO_2} are averaged values derived from triplicate experimental results.

The disintegration experiment is conducted in accordance with the ISO 16929-2021 test standard. The polymer film to be tested is in the shape of a square with dimensions of 2 cm × 2 cm and a thickness of 100 ± 30 μm. The polymer is buried at a depth of 20 cm in the compost soil at 58 ± 2 °C. After the disintegration, the mixture was screened to collect fragments larger than 2 mm, and the degree of disintegration was calculated (100%—mass of the collected fragments/mass of the sample before disintegration).

Toxicity assessment of compost soil: blank compost and sample compost were mixed with nutrient-rich humus soil at weight ratios of 25:75 or 50:50 (*w*/*w*) to cultivate 50 seeds each of radish and lettuce. The environmental temperature was maintained at 23–27 °C, with LED supplemental lighting providing a minimum of 16 h of daily illumination at an intensity of approximately 16,000 LUX. Seed germination rates were recorded after 24 days.

2.3. Synthesis of Polymers

PPC: The polymerization was conducted in the 50 mL autoclave. PPNCl (62 mg, 0.1 mmol), PO (5.8 g, 0.1 mol), and TEB (200 μL, 0.2 mmol) were sequentially added into the autoclave in the glove box. Then

the autoclave was sealed, removed from the glove box, and injected with 1 MPa CO_2. After the reaction remained for 4 h at 40 °C, the crude product was dissolved and diluted with CH_2Cl_2. The polymer was precipitated in 10-fold ethanol. The precipitate was collected and dried under vacuum at 80 °C until a constant weight was achieved.

PPCP: On the basis of PPC synthesis, a third monomer (PA) was added into the system to form PPCP-1 via a one-pot, one-step method. PPNCl (62 mg, 0.1 mmol), PA (3.7 g, 0.025 mol), PO (10.4 g, 0.18 mol) and TEB (200 µL, 0.2 mmol) were added to the autoclave sequentially. Reaction was conducted under 1 MPa CO_2, 70 °C for 4 h with magnetic stirring.

PPCX: Introduce CHO into the PPCP synthesis to synthesize PPCX-1. Added PPNCl (62 mg, 0.1 mmol), PA (7.4 g, 0.05 mol), PO (23.2 g, 0.4 mol), CHO (9.8 g, 0.1 mol) and TEB (200 µL, 0.2 mmol). The reaction was conducted under 1 MPa CO_2 at 68 °C for 5.5 h with magnetic stirring.

PPCPLA: Introduce PLA into PPCP synthesis. Added PPNCl (62 mg, 0.1 mmol), PA (3.7 g, 0.025 mol), PO (11.6 g, 0.2 mol), PLA (1 g, 0.1 g/mL in THF) and TEB (200 µL, 0.2 mmol). The reaction was conducted under 1 MPa CO_2 at 65 °C for 6 h with magnetic stirring.

3. Results and Discussion

3.1. Synthesis of CO_2-Derived Polymers

As a representative CO_2-derived polymer, poly(propylene carbonate) (PPC) is well-documented for its biodegradability. In this study, PPC was synthesized via a metal-free catalytic route and served as a reference material for comparative structural analysis with the newly developed CO_2-based polymers (see Supplementary Materials, Figures S1 and S2). Previous studies indicate that polycarbonates derived from sterically hindered epoxides and CO_2 exhibit retarded degradation kinetics [35,36]. To balance performance with biodegradability, we preserved the PPC backbone while strategically introducing polyester segments, aiming to enhance material properties without significantly compromising degradation capacity. Structural characterization of the resulting polymers is summarized in Figure 1 and Table 1.

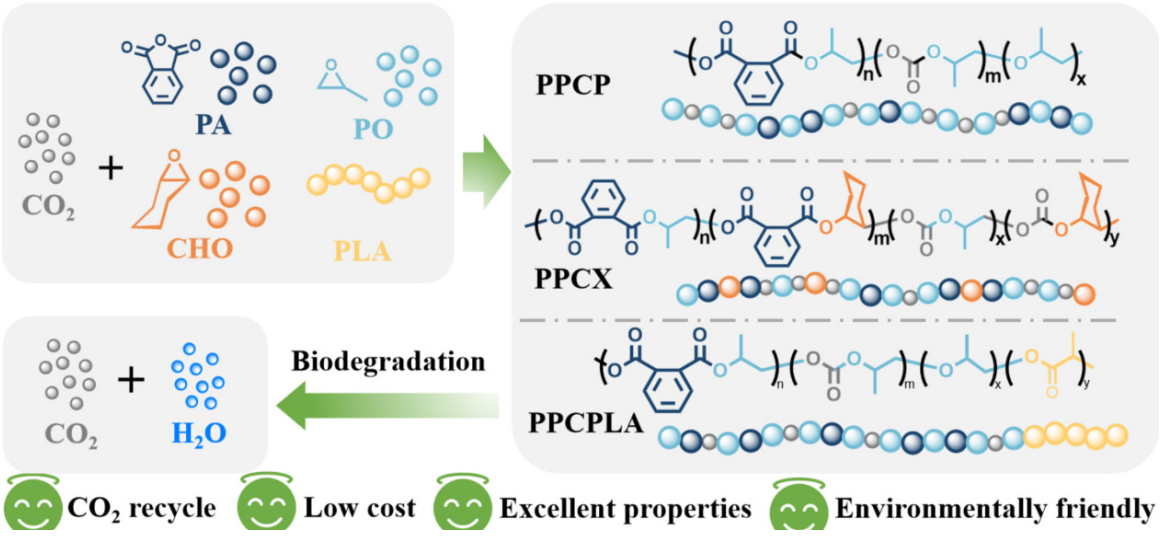

Figure 1. Structural architectures of CO_2-derived polymers are investigated in this work.

Initial copolymerization with phthalic anhydride (PA), a rigid aromatic monomer, yielded a polyester-polycarbonate copolymer (PPCP) with partial aromatic content. During the conventional propylene oxide (PO)/CO_2 alternating copolymerization, PA competes with CO_2 for insertion. The ^{1}H NMR spectrum of PPCP-1 (Figure 2a) shows characteristic signals at 5.4 ppm and 5.1 ppm, corresponding to the PA-alt-PO and CO_2-alt-PO repeating units, respectively. Through comprehensive structural analysis [15], we

confirmed that the resulting copolymer exhibits a random poly(ester-co-carbonate) architecture. Under optimized reaction conditions, undesirable side reactions—including PO homopolymerization and cyclic carbonate formation—were effectively suppressed, achieving high selectivity (≥93%) and minimal polyether content (≤2 wt%). Gel permeation chromatography (GPC) analysis revealed that PPCP-1 has a number-average molecular weight (M_n) of 49 kDa and a bimodal, narrow molecular weight distribution (Đ = 1.35), which can be attributed to residual terephthalic acid in PA acting as an additional initiator (Figure S3).

Thermal properties correlated with polyester content: PPCP-1 and PPCP-2 exhibited comparable molecular weights (M_n = 49 and 59 kDa, respectively) but distinct polyester mass fractions (52% and 62%) through controlled PA feed adjustment. Moreover, a hyperbranched analogue, PPCP-3, was synthesized using pyromellitic dianhydride (PMDA) as a chain extender, yielding an ultra-high molecular weight (M_n = 341 kDa). Its GPC profile displayed complex elution behavior and broad dispersity (Đ = 5.94), consistent with a branched polymer architecture.

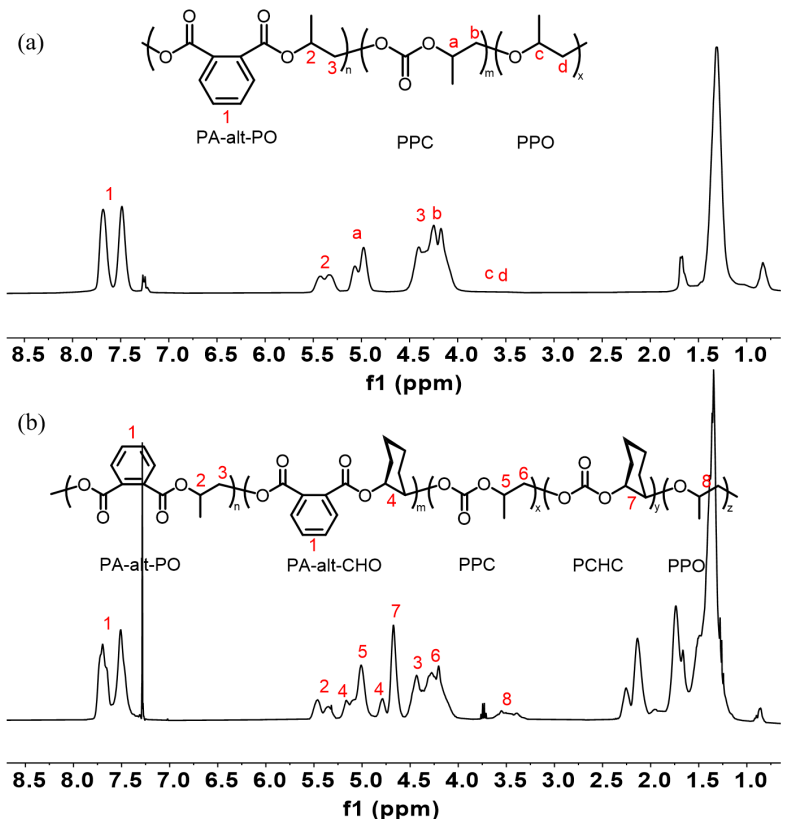

Figure 2. ^{1}H NMR spectrum of synthesized (**a**) PPCP-1 and (**b**) PPCX-1.

To enhance rigidity and increase the glass transition temperature (T_g), cyclohexene oxide (CHO) was introduced during PPCP synthesis, yielding a quaternary copolymer (PPCX) via competitive epoxide ring-opening [37]. This copolymer comprises four primary repeating units (Figure 2b): PA-alt-CO_2, PA-alt-CHO (contributing to polyester segments), and CO_2-alt-PO/CO_2-alt-CHO (constituting polycarbonate segments). Kinetic analysis indicated that anhydride–epoxide copolymerization proceeds more rapidly than epoxide–CO_2 copolymerization. Consequently, ester bond formation predominates in the early reaction stage, while carbonate bond generation becomes dominant later. By extending the reaction time under a feed ratio of PO/PA/CHO = 3000/500/1000, the polyester content was reduced from 51% to 46%. Gel permeation chromatography (GPC) traces of PPCX closely resembled those of PPCP (Figure S4), reflecting their analogous polymerization mechanisms.

Furthermore, transesterification of PPCP with polylactic acid (PLA) was employed to generate block copolymers (PPCPLA; Figure S5). This strategy synergistically retains the biodegradability of the parent

polymers while enhancing mechanical performance. The introduction of PLA segments specifically aims to increase the Vicat softening temperature (VST) of the material. Similar to the elevation of T_g, an increased VST is essential to expand the application window of these copolymers into environments requiring higher thermal stability.

Table 1. Copolymerization results of CO_2-derived polymers.

Sample	Material [a]	Ratio [b]	T (°C) [c]	t (h)	Conv. (%) [d]	Select. (%) [e]	PE/PC/PPO (*wt* %) [f]	M_n (10^3) [g]	Đ [g]
PPC	PO	1000	40	4	73	98	0/99/1	65	1.18
PPCP-1	PO/PA	1800/250	70	4	35	93	52/47/1	49	1.35
PPCP-2	PO/PA	1800/280	70	4.2	42	95	62/37/1	59	1.34
PPCP-3	PO/PA/PMDA	3200/450/3	65	4.1	65	93	55/43/1	341 [h]	5.94
PPCX-1	PO/PA/CHO	3000/500/1000	68	5.5	21/43 [i]	91	51/26/22/1 [j]	55	1.26
PPCX-2	PO/PA/CHO	3000/500/1000	68	7.5	25/46 [i]	89	46/29/23/2 [j]	61	1.26
PPCPLA	PO/PA	2000/250	70	6	37	95	36/9/52/3 [k]	37	1.28

[a] Main feed material, detailed compositions are described in the experimental section. [b] Molar ratio of material relative to the initiator. [c] Reaction temperature. [d] Conversion rate of PO calculated by ^{1}H NMR, except special instruction. [e] Calculated by ^{1}H NMR, selectivity = n (PO in polymer)/n (PO consumed). [f] Mass fraction of each unit in polymers except special instruction. Determined from ^{1}H NMR spectrum. PE = polyester, PC = polycarbonate, PPO = polypropylene oxide. [g] Determined by GPC in tetrahydrofuran with polystyrene standards except special instruction. [h] Determined by GPC in chloroform. [i] Conversion rate of PO/CHO. [j] Mass fraction of PE/PPC/PCHC/PPO. PE consists of poly(PA-alt-PO) and poly(PA-alt-CHO). [k] Mass fraction of PE/PLA/PPC/PPO. PE = poly(PA-alt-PO).

3.2. Properties of CO_2-Derived Polymers

Multicomponent copolymerization strategies fundamentally enhance the thermal and mechanical properties of PPC at the molecular level, as confirmed by comprehensive characterization data (Table 2, Figures S7–S14). The incorporation of rigid PA-alt-PO segments elevates the glass transition temperature (T_g) of PPCP to a range of 46–53 °C, compared to 38 °C for pure PPC, thereby addressing its inherent limitation for room-temperature applications. Systematic modulation of T_g was achieved by controlling polyester content, with PPCP-2 (52 °C at 62% polyester) demonstrating a near-linear correlation between aromatic content and thermal transition temperature (Figure S8). Thermogravimetric analysis (TG) revealed exceptional thermal stability across PPCP variants, with 5% weight loss temperatures (T_5%) exceeding 255 °C (range: 256–263 °C) and maximum decomposition temperatures (Tmax) reaching up to 369 °C (Table 2). Mechanical testing confirmed a substantial reinforcement effect, with tensile strength increasing from 29.6 MPa (PPC) to 38.9 MPa (PPCP-3). However, this enhancement in rigidity was accompanied by a trade-off in ductility, as indicated by reduced strain-at-break values below 10% (range: 7.2–8.4%), consistent with rigid thermoplastic behavior.

Table 2. Properties of synthesized CO_2-derived polymers.

Sample	T_g (°C) [a]	VST (°C)	T_{d5} (°C) [b]	T_{dmax} (°C) [b]	σ (MPa) [c]	ξ (%) [d]
PPC	38	36	236	246	29.6	56
PPCP-1	46	45	256	265, 361	34.4	7.2
PPCP-2	52	49	261	269, 365	38.3	8.4
PPCP-3	53	51	263	279, 369	38.9	7.6
PPCX-1	81	76	263	357	53.3	9.8
PPCX-2	75	73	273	359	47.2	14.8
PPCPLA	48, 169 [e]	52	224	258	35.1	6.6

[a] Determined at the second heating run by DSC. [b] Determined by TGA, T_{d5} = 5% weight loss temperature, T_{dmax} = maximum weight loss temperature. [c] Tensile strength. [d] Elongation at break. [e] 169 °C is crystallization melting temperature.

Processing characteristics also show significant variation. For instance, PPCP-2 exhibits a high melt flow index (MFI) of 53.8 g/10 min (190 °C, 2.16 kg; Figure S15), indicating a potential for flow instability during extrusion. In contrast, the hyperbranched PPCP-3 achieves optimized processability (MFI = 7.3 g/10 min) due to chain entanglement effects, while simultaneously maintaining an enhanced glass transition temperature (T_g = 53 °C *vs*. 48 °C for PPCP-2). Since the T_g of both PPCP-2 and PPCP-3 are above room temperature, these materials behave as rigid and brittle plastics. Consequently, no significant improvement in toughness (*i.e.*, elongation at break) was observed. This combination of favorable thermal stability (T_5% = 263 °C), mechanical strength (38.9 MPa), and processability positions PPCP as a promising, cost-effective alternative to commercial bioplastics.

Quaternary copolymers (PPCX series) exhibit superior performance metrics. Specifically, PPCX-1 achieves a record T_g of 81 °C through CHO incorporation, with a tensile strength of 53.3 MPa—approximately 40% higher than its PPCP counterparts. PPCX-2 demonstrates a balanced thermo-mechanical profile (T_g = 75 °C, strain at break = 14.8%), indicating potential suitability for dynamic load-bearing applications. Block copolymerization with PLA yields PPCPLA, which retains a T_g comparable to PPCP (48 °C) while introducing crystallinity, as evidenced by a melting temperature (Tm) of 169 °C (Figure S10). Despite a minimal increase in tensile strength (35.1 MPa *vs*. 34.4 MPa for PPCP-1), this crystalline-amorphous architecture elevates the Vicat softening temperature (VST) to 52 °C. Notably, the VST values for PPCP materials are typically slightly lower than their corresponding T_g values. This contrast suggests that PPCPLA offers a higher tolerable service and storage temperature range compared to its amorphous PPCP counterparts.

Collectively, these structure-property relationships confirm that strategic monomer selection and topological control—spanning linear, hyperbranched, and block architectures—enable precise tuning of CO_2-derived polymers to meet diverse application-specific and processing requirements.

3.3. Biodegradability Analysis of CO_2-Derived Polymers

The ultimate objective of polymer biodegradation is to completely degrade into water, CO_2, and non-toxic metabolites, without generating persistent microplastics—a critical advantage over petroleum-based counterparts, which can form ecotoxic nanoplastics through partial degradation [38]. To evaluate this process systematically, we conducted aerobic composting tests in accordance with ISO 14855, using an agricultural waste-derived inoculum. Biodegradation kinetics were quantified by gravimetric analysis of evolved CO_2 (see Experimental Section for detailed methodology). Figure 3a presents the biodegradation profiles of six CO_2-derived polymers over a 180-day period.

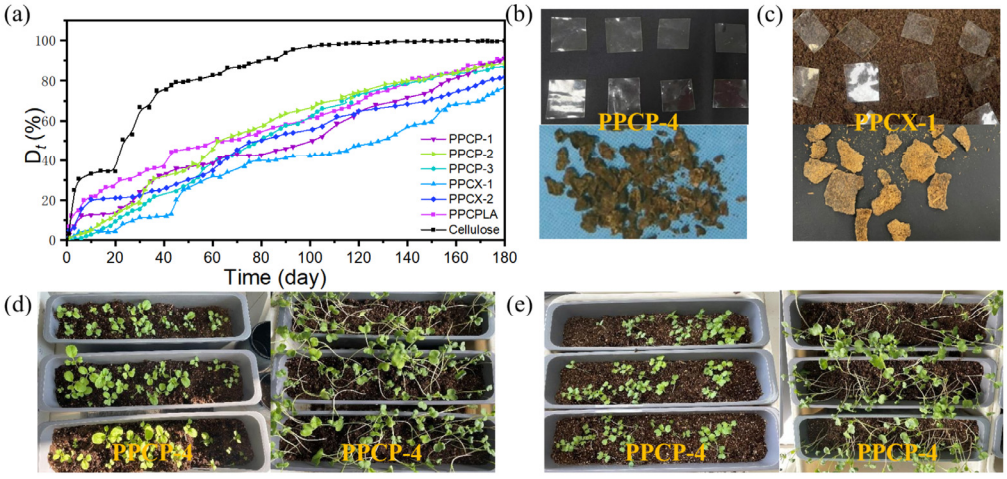

Figure 3. Results of biodegradation for synthesized CO_2-derived copolymers. (**a**) The biodegradation rate of the sample during 180 days' composting tests. (**b**) PPCP-2 after 12 weeks' disintegration experiment. (**c**) PPCX-1 after a 19 weeks' disintegration

experiment. The germination of lettuce (**left**) and radish (**right**) seeds under incorporating 25% of the compost soil from the (**d**) control group and (**e**) of PPCP-3 group.

The control material, thin-layer chromatography (TLC)-grade cellulose, reached biodegradation rates of 80% by day 55 and 99.9% by day 180. To facilitate a comprehensive comparison, we selected the biodegradation rates at day 45 (D45) and day 180 (D180) as key evaluation points; the corresponding data are detailed in Table S1. The time required to reach 90% biodegradation served as a primary metric for assessing overall degradation kinetics. All synthesized CO_2-derived copolymers exhibited stable degradation over 180 days. For PPCP-1, the D45 and D180 values were 35.9% and 90.9%, respectively. Increasing polyester content was found to influence the early-stage degradation rate. PPCP-2, with a polyester content of 62%, showed a slightly reduced D45 value of 33.5%. Despite this, both PPCP-1 and PPCP-2 achieved approximately 90% biodegradation by D180, confirming their excellent ultimate biodegradability.

The degradation rate of hyperbranched PPCP-3 was significantly lower in the early stage (D45 = 24.5%), a result attributed to stronger intermolecular chain interactions that hinder microbial access. Nonetheless, it surpassed 90% biodegradation by day 202. Given its favorable thermal, mechanical, and processing properties, PPCP-3 represents a promising candidate for broad application as a biodegradable plastic.

In contrast, the early biodegradation rates of PPCX-1 and PPCX-2 were notably lower than those of the PPCP series, with D45 values of 20.1% and 27.9%, respectively. Their corresponding degradation curves are positioned lower in Figure 3a. This retardation is due to the presence of PA-alt-CHO and CO_2-alt-CHO structural units, which introduce considerable steric hindrance and thus slow enzymatic attack. Importantly, because these units are randomly distributed within the copolymer, their negative impact on biodegradability remains acceptable when balanced against the enhanced thermal and mechanical performance they provide.

PPCPLA exhibited the fastest early-stage degradation, attributable to the well-known biodegradability of PLA. However, in later stages, its degradation rate converged with that of PPCP, likely due to the low PLA content (9%) in the copolymer.

Since the specific surface area of bulk plastic products is limited, microbial colonization significantly influences the biodegradation rate. Disintegration experiments on film materials provide a more realistic assessment of practical biodegradation. Films of PPCP-3 and PPCX-1 (2 cm × 2 cm × 100 μm) were subjected to compost disintegration, with their condition monitored over time (Figure 3b,c). PPCP-3 underwent water absorption, swelling, fragmentation, and pronounced surface erosion during composting, achieving 93.5% disintegration after 12 weeks. PPCX-1 reached 78.5% disintegration after 19 weeks. The slower disintegration of PPCX-1 aligns with the powder biodegradation results, confirming that rigid structural units with higher steric hindrance reduce the degradation rate.

While most biodegradable plastics rarely achieve complete mineralization under test conditions, the samples in this study all exceeded 90% biodegradation. This indicates that over 90% of the polymer's carbon completely degrades into water and CO_2. Since compost soils are commonly used in agriculture, seed germination tests were conducted to assess potential phytotoxicity. Lettuce and radish seeds were cultivated in mixtures of PPCP-3 compost soil and humus soil at ratios of 25:75 and 50:50 (*w*/*w*). As shown in Table S2 and Figure 3d,e, germination rates in sample and blank compost soils were nearly identical, confirming that no phytotoxic byproducts were generated during biodegradation.

This comprehensive degradation profile—characterized by high ultimate biodegradation, effective disintegration, and non-toxicity—allow CO_2-based polymers to expand their use in more sustainable material applications.

4. Conclusions

This study demonstrates that multicomponent copolymerization is an effective strategy for enhancing the thermal and mechanical properties of CO_2-derived polymers while preserving their biodegradability. The semi-aromatic polyester-polycarbonate PPCP achieves a glass transition temperature (T_g) of 52 °C and a tensile strength of 38.3 MPa, thereby addressing the key limitations of PPC for room-temperature applications. The hyperbranched derivative, PPCP-3, exhibits improved processability (MFI = 7.3 g/10 min) due to controlled chain extension, resolving the melt-flow instability observed in its linear analogs. The introduction of cyclohexene oxide (CHO) further elevates Tg to 81 °C (PPCX-1), enabling performance in higher-temperature environments. Meanwhile, the PPCPLA block copolymer not only retains excellent biodegradability but also achieves a higher upper service temperature, as confirmed by its elevated Vicat softening temperature (VST).

Under standard composting conditions, PPCP materials reach >90% biodegradation within 180 days and show complete non-toxicity to crops, with seed germination rates exceeding 88%. Relative to cellulose—a benchmark natural biodegradable polymer—these CO_2-derived copolymers exhibit comparable and commendable biodegradability. This integrated molecular design strategy, which successfully balances performance enhancement, microbial degradation pathways, and cost efficiency, provides a fairly satisfactory option for developing sustainable polymers. Future work will focus on industrial-scale production optimization and evaluating marine degradation profiles to advance applications in packaging, agricultural films, and medical disposables.

Supplementary Materials

The following supporting information can be found at: https://www.sciepublish.com/article/pii/1079, Figure S1: ^{1}H NMR spectrum of synthesized PPC; Figure S2: GPC curve for synthesized PPC; Figure S3: GPC curves for synthesized PPCP-1, PPCP-2 and PPCP-3; Figure S4: GPC curves for synthesized PPCX-1 and PPCX-2; Figure S5: ^{1}H NMR spectrum of synthesized PPCPLA; Figure S6: DSC curve for PPCPLA; Figure S7: DSC curve for synthesized PPC; Figure S8: DSC curves for synthesized PPCP; Figure S9: DSC curves for synthesized PPCX; Figure S10: DSC curve for synthesized PPCPLA; Figure S11: Stress-strain curve of synthesized PPC at a stretching rate of 50 mm/min; Figure S12: Stress-strain curves of synthesized PPCP at a stretching rate of 5 mm/min; Figure S13: Stress-strain curves of synthesized PPCX at a stretching rate of 5 mm/min; Figure S14: Stress-strain curve of synthesized PPCPLA at a stretching rate of 50 mm/min; Figure S15: MFI of synthesized PPCP-2 and PPCP-4; Table S1: Results of biodegradation for synthesized CO_2-derived copolymers; Table S2: Germination results of lettuce and radish seeds in sample compost and blank compost soils [a].

Statement of the Use of Generative AI and AI-Assisted Technologies in the Writing Process

During the preparation of this manuscript, the authors used Deepseek in order to translation and polishing of expressions. After using this tool, the authors reviewed and edited the content as needed and take full responsibility for the content of the published article.

Acknowledgments

The authors extend gratitude to the Collaborative Innovation Center for NQI-Quality Safety of Guangzhou (No. 2023B04J0407) and Guangzhou Academician and Expert Workstation (No. 2024-D012).

Author Contributions

Conceptualization, Y.R. and M.X.; Methodology Y.R. and X.Z.; Validation, D.H., S.H. and S.W.; Investigation, Y.R.; Resources, M.X.; Data Curation, D.H.; Writing—Original Draft Preparation, Y.R.; Writing—Review & Editing, X.Z. and M.X.; Funding Acquisition, M.X.

Ethics Statement

Not applicable.

Informed Consent Statement

Not applicable.

Data Availability Statement

The data supporting the findings of this study are available from the corresponding author upon reasonable request.

Funding

This work was financially supported by the Collaborative Innovation Center for NQI-Quality Safety of Guangzhou (No. 2023B04J0407) and Guangzhou Academician and Expert Workstation (No. 2024-D012).

Declaration of Competing Interest

The authors declare that they have no known competing financial interests or personal relationships that could have appeared to influence the work reported in this paper.

References

1. van Veelen B, Hasselbalch J. Power and politics in plastics research: A critique of "Whither Plastics". *Energy Res. Soc. Sci.* **2020**, *61*, 101445. DOI:10.1016/j.erss.2020.101445
2. Bahuleyan BK, Park DW, Ha CS, Kim I. Advances in late transition metal catalysts for olefin polymerization/oligomerizarion. *Catal. Surv. Asia* **2006**, *10*, 65–73. DOI:10.1007/s10563-006-9008-7
3. Andrady AL. Microplastics in the marine environment. *Mar. Pollut. Bull.* **2011**, *62*, 1596–1605. DOI:10.1016/j.marpolbul.2011.05.030
4. Lim BKH, Thian ES. Biodegradation of polymers in managing plastic waste—A review. *Sci. Total Environ.* **2022**, *813*, 151880. DOI:10.1016/j.scitotenv.2021.151880
5. Zheng Y, Yanful EK, Bassi AS. A Review of Plastic Waste Biodegradation. *Crit. Rev. Biotechnol.* **2005**, *25*, 243–250. DOI:10.1080/07388550500346359
6. Nizamuddin S, Baloch AJ, Chen C, Arif M, Mubarak NM. Bio-based plastics, biodegradable plastics, and compostable plastics: Biodegradation mechanism, biodegradability standards and environmental stratagem. *Int. Biodeterior. Biodegrad.* **2024**, *195*, 105887. DOI:10.1016/j.ibiod.2024.105887
7. Kumar R, Sadeghi K, Jang J, Seo J. Mechanical, chemical, and bio-recycling of biodegradable plastics: A review. *Sci. Total Environ.* **2023**, *882*, 163446. DOI:10.1016/j.scitotenv.2023.163446
8. Jia M, Zhang D, Gnanou Y, Feng X. Surfactant-Emulating Amphiphilic Polycarbonates and Other Functional Polycarbonates through Metal-Free Copolymerization of CO_2 with Ethylene Oxide. *ACS Sustain. Chem. Eng.* **2021**, *9*, 10370–10380. DOI:10.1021/acssuschemeng.1c03751
9. Siragusa F, Detrembleur C, Grignard B. The advent of recyclable CO_2-based polycarbonates. *Polym. Chem.* **2023**, *14*, 1164–1183. DOI:10.1039/D2PY01258H
10. Zhang D, Boopathi SK, Hadjichristidis N, Gnanou Y, Feng X. Metal-Free Alternating Copolymerization of CO_2 with Epoxides: Fulfilling "Green" Synthesis and Activity. *J. Am. Chem. Soc.* **2016**, *138*, 11117–11120. DOI:10.1021/jacs.6b06679

11. Holzmüller P, Gardiner C, Preis J, Frey H. CO_2-Based Polycarbonates with Low Glass Transition Temperatures Sourced from Long-Chain Terpenes. *Macromolecules* **2024**, *57*, 5358–5367. DOI:10.1021/acs.macromol.4c00349
12. Ren Y, Zhang T, Wang S, Han D, Huang S, Guo H, et al. CO_2 derived ABA triblock all-polycarbonate thermoplastic elastomer with ultra-high elastic recovery. *J. CO_2 Util.* **2024**, *85*, 102853. DOI:10.1016/j.jcou.2024.102853
13. Inoue S, Koinuma H, Tsuruta T. Copolymerization of carbon dioxide and epoxide. *J. Polym. Sci. B Polym. Lett.* **1969**, *7*, 287–292. DOI:10.1002/pol.1969.110070408
14. Jia M, Hadjichristidis N, Gnanou Y, Feng X. Monomodal Ultrahigh-Molar-Mass Polycarbonate Homopolymers and Diblock Copolymers by Anionic Copolymerization of Epoxides with CO_2. *ACS Macro Lett.* **2019**, *8*, 1594–1598. DOI:10.1021/acsmacrolett.9b00854
15. Liang J, Ye S, Wang W, Fan C, Wang S, Han D, et al. Performance tailorable terpolymers synthesized from carbon dioxide, phthalic anhydride and propylene oxide using Lewis acid-base dual catalysts. *J. CO_2 Util.* **2021**, *49*, 101558. DOI:10.1016/j.jcou.2021.101558
16. Liang J, Ye S, Wang S, Wang S, Han D, Huang S, et al. Biodegradable Copolymers from CO_2, Epoxides, and Anhydrides Catalyzed by Organoborane/Tertiary Amine Pairs: High Selectivity and Productivity. *Macromolecules* **2022**, *55*, 6120–6130. DOI:10.1021/acs.macromol.2c01118
17. Darensbourg DJ, Poland RR, Escobedo C. Kinetic Studies of the Alternating Copolymerization of Cyclic Acid Anhydrides and Epoxides, and the Terpolymerization of Cyclic Acid Anhydrides, Epoxides, and CO_2 Catalyzed by (salen)CrIIICl. *Macromolecules* **2012**, *45*, 2242–2248. DOI:10.1021/ma2026385
18. Ji HY, Wang B, Pan L, Li YS. Lewis pairs for ring-opening alternating copolymerization of cyclic anhydrides and epoxides. *Green Chem.* **2018**, *20*, 641–648. DOI:10.1039/C7GC03261G
19. Paul S, Zhu Y, Romain C, Brooks R, Saini PK, Williams CK. Ring-opening copolymerization (ROCOP): Synthesis and properties of polyesters and polycarbonates. *Chem. Commun.* **2015**, *51*, 6459–6479. DOI:10.1039/C4CC10113H
20. Liu Y, Wu J, Hu X, Zhu N, Guo K. Advances, Challenges, and Opportunities of Poly(γ-butyrolactone)-Based Recyclable Polymers. *ACS Macro Lett.* **2021**, *10*, 284–296. DOI:10.1021/acsmacrolett.0c00813
21. Song P, Xu H, Mao X, Liu X, Wang L. A one-step strategy for aliphatic poly(carbonate-ester)s with high performance derived from CO_2, propylene oxide andl-lactide. *Polym. Adv. Technol.* **2017**, *28*, 736–741. DOI:10.1002/pat.3974
22. Liu Y, Huang K, Peng D, Wu H. Synthesis, characterization and hydrolysis of an aliphatic polycarbonate by terpolymerization of carbon dioxide, propylene oxide and maleic anhydride. *Polymer* **2006**, *47*, 8453–8461. DOI:10.1016/j.polymer.2006.10.024
23. Duan Z, Wang X, Gao Q, Zhang L, Liu B, Kim I. Highly active bifunctional cobalt-salen complexes for the synthesis of poly(ester-*block*-carbonate) copolymer*via*terpolymerization of carbon dioxide, propylene oxide, and norbornene anhydride isomer: Roles of anhydride conformation consideration. *J. Polym. Sci. Part A Polym. Chem.* **2014**, *52*, 789–795. DOI:10.1002/pola.27057
24. Deng K, Wang S, Ren S, Han D, Xiao M, Meng Y. A Novel Single-Ion-Conducting Polymer Electrolyte Derived from CO2-Based Multifunctional Polycarbonate. *ACS Appl. Mater. Interfaces* **2016**, *8*, 33642–33648. DOI:10.1021/acsami.6b11384
25. Liu Y, Deng K, Wang S, Xiao M, Han D, Meng Y. A novel biodegradable polymeric surfactant synthesized from carbon dioxide, maleic anhydride and propylene epoxide. *Polym. Chem.* **2015**, *6*, 2076–2083. DOI:10.1039/C4PY01801J
26. Kim MC, Masuoka T. A study on the degradation property of a hydrophilic polycarbonate film treated by inductively coupled plasma using CO_2 as reactive gas. *Appl. Surf. Sci.* **2009**, *255*, 4684–4688. DOI:10.1016/j.apsusc.2008.12.027
27. Liao X, Cui FC, He JH, Ren WM, Lu XB, Zhang YT. A sustainable approach for the synthesis of recyclable cyclic CO_2-based polycarbonates. *Chem. Sci.* **2022**, *13*, 6283–6290. DOI:10.1039/D2SC01387H
28. Song P, Mao X, Zhang X, Zhu X, Wang R. A one-step strategy for cross-linkable aliphatic polycarbonates with high degradability derived from CO_2, propylene oxide and itaconic anhydride. *RSC Adv.* **2014**, *4*, 15602–15605. DOI:10.1039/C4RA01514B
29. Zheng X, Wang W, Cui Y, Jia X, Li H, Liu X, et al. Degradable Pressure-Sensitive Adhesive Prepared From CO_2-Based Polycarbonate. *J. Polym. Sci.* **2025**, *63*, 864–875. DOI:10.1002/pol.20240965
30. Huang X, Zhao T, Wang S, Han D, Huang S, Guo H, et al. Self-Healable, Transparent, Biodegradable, and Shape Memorable Polyurethanes Derived from Carbon Dioxide-Based Diols. *Molecules* **2024**, *29*, 4364. DOI:10.3390/molecules29184364
31. Zhao T, Chen S, Huang X, Yin J, Wang S, Han D, et al. Metal-Free Synthesis of Biodegradable CO_2-Based Oligo(carbonate-ester) Diols as Building Blocks for Thermoplastic Polyurethanes. *ACS Appl. Polym. Mater.* **2024**, *6*, 1813–1822. DOI:10.1021/acsapm.3c02652

32. Huang X, Alferov K, Zhao T, Yin J, Wang S, Han D, et al. Facile and direct synthesis of oligocarbonate diols from carbon dioxide and their application as sustainable feedstock for polyurethane. *J. CO_2 Util.* **2023**, *75*, 102571. DOI:10.1016/j.jcou.2023.102571
33. Chen S, Zhao T, Li P, Wang S, Han D, Huang S, et al. Biodegradable PVC plasticizer derived from a new CO_2-based Poly(carbonate-ester) macrodiol: Molecular design and plasticizing effect. *J. CO_2 Util.* **2024**, *80*, 102695. DOI:10.1016/j.jcou.2024.102695
34. Wang WJ, Ye SX, Liang JX, Fan CX, Zhu YL, Wang SJ, et al. Architecting Branch Structure in Terpolymer of CO_2, Propylene Oxide and Phthalic Anhydride: An Enhancement in Thermal and Mechanical Performances. *Chin. J. Polym. Sci.* **2022**, *40*, 462–468. DOI:10.1007/s10118-022-2686-4
35. Du LC, Meng YZ, Wang SJ, Tjong SC. Synthesis and degradation behavior of poly(propylene carbonate) derived from carbon dioxide and propylene oxide. *J. Appl. Polym. Sci* **2004**, *92*, 1840–1846. DOI:10.1002/app.20165
36. Varghese JK, Na SJ, Park JH, Woo D, Yang I, Lee BY. Thermal and weathering degradation of poly(propylene carbonate). *Polym. Degrad. Stab.* **2010**, *95*, 1039–1044. DOI:10.1016/j.polymdegradstab.2010.03.006
37. Ye S, Wang W, Liang J, Wang S, Xiao M, Meng Y. Metal-Free Approach for a One-Pot Construction of Biodegradable Block Copolymers from Epoxides, Phthalic Anhydride, and CO_2. *ACS Sustain. Chem. Eng.* **2020**, *8*, 17860–17867. DOI:10.1021/acssuschemeng.0c07283
38. Qin M, Chen C, Song B, Shen M, Cao W, Yang H, et al. A review of biodegradable plastics to biodegradable microplastics: Another ecological threat to soil environments? *J. Clean. Prod.* **2021**, *312*, 127816. DOI:10.1016/j.jclepro.2021.127816